BULLETIN OF THE POLISH ACADEMY OF SCIENCES
TECHNICAL SCIENCES, Vol. 60, No. 1, 2012
DOI: 10.2478/v10175-012-0020-y

Rapid antenna design optimization using shape-preserving response prediction

S. KOZIEL[1]*, S. OGURTSOV[1], and S. SZCZEPANSKI[2]

[1] Engineering Optimization & Modeling Center, School of Science and Engineering, Reykjavík University
Menntavegur 1, 101 Reykjavík, Iceland
[2] Department of Microelectronic Systems, Gdansk University of Technology, 11/12 G. Narutowicza St., 80-952 Gdansk, Poland

Abstract. An approach to rapid optimization of antennas using the shape-preserving response-prediction (SPRP) technique and coarse-discretization electromagnetic (EM) simulations (as a low-fidelity model) is presented. SPRP allows us to estimate the response of the high-fidelity EM antenna model, e.g., its reflection coefficient versus frequency, using the properly selected set of so-called characteristic points of the low-fidelity model response. The low-fidelity model, corrected by means of SPRP, is subsequently used to predict the optimal design. The design process is cost efficient because most operations are performed on the low-fidelity model. Performance of our technique is demonstrated using a dielectric resonator antenna and two planar wideband antenna examples. In all cases, the optimal design is obtained at a cost corresponding to a few high-fidelity simulations of the antenna under design.

Key words: antenna design, simulation-driven design, antenna optimization, shape-preserving response prediction, coarse-discretization simulation.

1. Introduction

Design of antenna structures normally involves adjustment of geometry parameters so that various requirements imposed on the impedance bandwidth and radiation figures should be satisfied. In many cases, such an optimization process necessarily includes repetitive high-fidelity electromagnetic (EM) simulations. The primary reason for the use of such simulations is that "in practice" analytical models, if available, can only yield initial designs that need to be further tuned to meet design requirements [1–4]. Also interactions between the antenna and its environment, e.g., feeding circuits, connectors, installation platforms, device housing, etc. [1], affect the antenna operation and have to be taken into account in the design process. As a result, simulation-based antenna design becomes increasingly important. As a matter of fact, it might be the only systematic option for modern types of ultrawideband (UWB) antennas [1, 3] and dielectric resonator antennas (DRAs) [2] where no straightforward procedures are available that would result in antenna designs with prescribed reflection and radiation responses.

Although necessary, EM-simulation-driven design may be quite challenging. Perhaps the most fundamental obstacle is a high-computational cost of accurate, high-fidelity antenna simulation (up to a few hours per geometry). In particular, straightforward design automation approaches by employing the discrete EM solver directly in an optimization loop are often turns to be impractical because conventional optimization algorithms require large numbers of objective function evaluations [5]. Numerical noise, which is always present in EM-simulated responses, makes the problem even less feasible with the gradient-based algorithms.

Various meta-heuristic approaches have also been applied to antenna design, including genetic algorithms [6–9], particle swarm optimizers [10–12], or ant colony systems [13]. Although these methods have certain advantages (e.g., handling non-differentiable and multi-modal functions, global search capability), they normally require massive amounts of function evaluations and, therefore, are not recommended when high-fidelity EM simulations are used. It is worth to mention that, differently from the technique presented in this paper, the meta-heuristic algorithms do not alleviate the costs of simulations embedded into the optimization loop.

The efficient simulation-driven design can be realized using the surrogate-based optimization (SBO) concept [14, 15]. In SBO, the optimization burden is shifted to a surrogate model, computationally cheap representation of the optimized structure. There are two basic approaches to build the surrogate model: (i) approximation of the high-fidelity model data (using, e.g., neural networks [16, 17], support-vector regression [18, 19], fuzzy systems [20, 21], Cauchy approximation [22], or kriging [23, 24]), and (ii) suitable correction of a physics-based low-fidelity model (e.g., space mapping (SM) [25–27], tuning [28, 29]). Approximation models are quite versatile; however, they also require large sets of training data which are normally acquired with substantial computational effort. This sort of investment is justified for the multiple use library models [16] but not quite for ad-hoc optimization. On the other hand, reasonably accurate physics-based surrogates can be created using a limited number of training points [25]; in some cases, even a single high-fidelity simulation can be sufficient [30].

*e-mail: koziel@ru.is

Unfortunately, techniques such as space mapping and tuning are not very suitable for antenna design. Space mapping relies on a fast coarse model, typically, a circuit equivalent [25, 27], whereas reliable circuit equivalents are not available for many important types of antenna, e.g., for DRAs [1, 2], UWB antennas [1, 3], and Yagi antennas [1, 4]. On the other hand, simulation-based tuning is not directly applicable for radiating structures.

In this paper, to realize computationally efficient antenna design, we adopt a recently published shape-preserving response prediction (SPRP) technique [30]. SPRP is utilized to create a reliable surrogate model of the antenna by aligning the simulation results of its coarsely-discretized model (low-fidelity model) with that obtained through high-fidelity EM simulation. The surrogate serves as a prediction tool that estimates the optimal geometry of the high-fidelity model. In this correction-prediction scheme, most of the operations are performed on the coarse-discretization model so that the total design cost is low and typically corresponds to a few evaluations of the high-fidelity antenna model. Also, unlike space mapping, SPRP does not use a parameter extraction step, which allows us to maintain low design costs even if the low-fidelity antenna model is relatively expensive. Our approach is demonstrated through the design of two wideband planar antennas and a dielectric resonator antenna.

2. Antenna design using shape-preserving response prediction

In this section, we formulate the antenna design problem, discuss the generic surrogate-based optimization algorithm, as well as describe the SPRP technique.

2.1. Formulation of the design problem. It is convenient to formulate the antenna design task as a nonlinear minimization problem of the form

$$\boldsymbol{x}_f^* = \arg\min_{\boldsymbol{x}} U\left(\boldsymbol{R}_f(\boldsymbol{x})\right), \tag{1}$$

where $\boldsymbol{R}_f(\boldsymbol{x}) \in R^m$ denotes the response vector, e.g., $|S_{11}|$ over a frequency range of interest, evaluated using accurate full-wave EM simulation; $\boldsymbol{x} \in R^n$ is a vector of design variables (e.g., relevant geometry parameters of the antenna); U is a given objective function (e.g., typically minimax [5]) defined so that better design $\boldsymbol{x}$ corresponds to smaller values of $U(\boldsymbol{R}(\boldsymbol{x}))$.

2.2. Surrogate-based optimization. We assume that high-fidelity EM simulation of the optimized antenna is computationally expensive so that solving (1) directly is impractical. Instead, we would like to use the surrogate-based optimization (SBO) approach [14, 15, 24], where a sequence of approximate solutions to (1) is obtained using the iterative procedure:

$$\boldsymbol{x}^{(i+1)} = \arg\min_{\boldsymbol{x}} U\left(\boldsymbol{R}_s^{(i)}(\boldsymbol{x})\right). \tag{2}$$

Here, $\boldsymbol{R}_s^{(i)}$ is the surrogate model at iteration i, whereas $\boldsymbol{x}^{(i+1)}$ is the approximate solution to (1) obtained by optimizing $\boldsymbol{R}_s^{(i)}$. The surrogate is constructed using the low-fidelity model $\boldsymbol{R}_c$: a less accurate but computationally cheap representation of the high-fidelity model $\boldsymbol{R}_f$.

The main idea behind (2) is that – for a properly working SBO algorithm – the high-fidelity model is only evaluated a few times (preferably even once) per iteration, and the surrogate model is fast. As a result, the overall computational cost of the SBO process (2) might be substantially lower than the cost of solving (1) directly using any conventional (e.g., gradient-based) optimization algorithm.

2.3. Coarse-discretization electromagnetic models. The SBO techniques might be particularly efficient with the physics-based low-fidelity models such as space mapping [25, 27] or simulation-based tuning [29]. However, the area of application of these methods is limited to the problems where fast circuit equivalents are readily available, e.g., in the case of microstrip filters [25–27]. In antenna design, reliable analytical or circuit models are often unavailable, particularly for DRA antennas [2].

The realization of the SBO concept for the antenna design requires another type of low-fidelity models. The only versatile candidate seems to be the low-fidelity model which is originated from coarse-discretization EM simulations. This type of low-fidelity model is universally available since it can be implemented with the same solver as the one evaluating the high-fidelity model by applying relaxed mesh requirements. One disadvantage of the coarse-discretization models is that they are relatively expensive: typically, the evaluation time ratio of the high- and low-fidelity model spans from 5 to 50. This means that any algorithm exploiting coarse-discretization models should be designed to reduce not only the number of high-fidelity model evaluations but also low-fidelity ones. With this respect, space mapping may not be a good choice because of its parameter extraction step [5], which typically requires a large number of low-fidelity model calls.

2.4. Shape-Preserving Response Prediction (SPRP). Here, we construct the surrogate model for the SBO scheme (2) using the SPRP technique [30]. Unlike space mapping, SPRP does not use any extractable parameters and it is typically very efficient: in many cases [30] only two or three iterations are sufficient to yield a satisfactory design.

SPRP assumes that the change of the high-fidelity model response due to the adjustment of the design variables can be predicted using the actual changes of the low-fidelity model response. Here, this property is ensured by the low-fidelity model being the coarse-mesh simulation of the same structure that represents the high-fidelity model.

The change of the low-fidelity model response can be described by the translation vectors corresponding to so-called characteristic points of the model's response. These translation vectors are subsequently used to predict the change of the high-fidelity model response with the actual response of $\boldsymbol{R}_f$ at the current iteration point, $\boldsymbol{R}_f(\boldsymbol{x}^{(i)})$, treated as a reference.

Figure 1a shows an example low-fidelity model response, $|S_{11}|$ versus frequency, at the design $\boldsymbol{x}^{(i)}$, as well as the

coarse model response at some other design $\boldsymbol{x}$. The responses come from the dielectric resonator antenna considered in Subsec. 3.1. Circles denote characteristic points of $\boldsymbol{R}_c(\boldsymbol{x}^{(i)})$, selected here to represent $|S_{11}| = -10$ dB, $|S_{11}| = -15$ dB, and the local $|S_{11}|$ minimum. Squares denote corresponding characteristic points for $\boldsymbol{R}_c(\boldsymbol{x})$, while line segments represent the translation vectors ("shift") of the characteristic points of $\boldsymbol{R}_c$ when changing the design variables from $\boldsymbol{x}^{(i)}$ to $\boldsymbol{x}$.

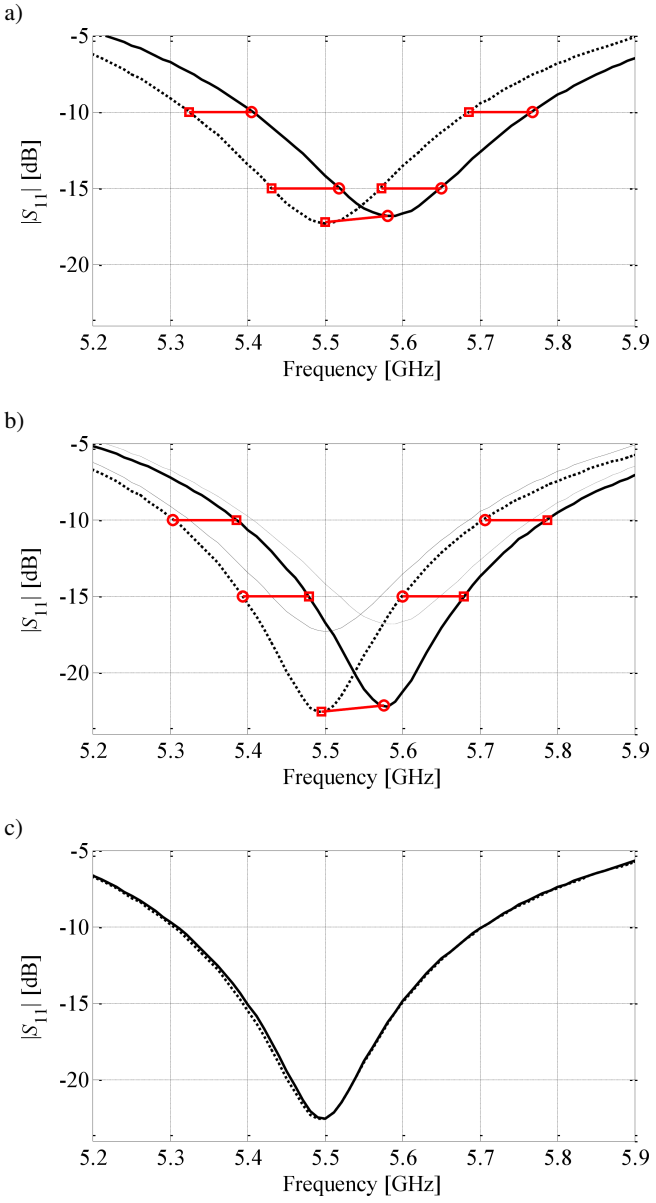

Fig. 1. SPRP concept: a) Low-fidelity model response at the design $\boldsymbol{x}^{(i)}$, $\boldsymbol{R}_c(\boldsymbol{x}^{(i)})$ (solid line), the low-fidelity model response at $\boldsymbol{x}$, $\boldsymbol{R}_c(\boldsymbol{x})$ (dotted line), characteristic points of $\boldsymbol{R}_c(\boldsymbol{x}^{(i)})$ (circles) and $\boldsymbol{R}_c(\boldsymbol{x})$ (squares), and the translation vectors (short lines); b) high-fidelity model response at $\boldsymbol{x}^{(i)}$, $\boldsymbol{R}_f(\boldsymbol{x}^{(i)})$ (solid line) and the predicted high-fidelity model response at $\boldsymbol{x}$ (dotted line) obtained using SPRP based on characteristic points of Fig. 1a; characteristic points of $\boldsymbol{R}_f(\boldsymbol{x}^{(i)})$ (circles) and the translation vectors (short lines) were used to find the characteristic points (squares) of the predicted high-fidelity model response; low-fidelity model responses $\boldsymbol{R}_c(\boldsymbol{x}^{(i)})$ and $\boldsymbol{R}_c(\boldsymbol{x})$ are plotted using thin solid and dotted line, respectively

The high-fidelity model response at $\boldsymbol{x}$ can be predicted using the same translation vectors applied to the corresponding characteristic points of the high-fidelity model response at $\boldsymbol{x}^{(i)}$, $\boldsymbol{R}_f(\boldsymbol{x}^{(i)})$. This is illustrated in Fig. 1b. Figure 1c shows the predicted high-fidelity model response and the actual high-fidelity model response at $\boldsymbol{x}$. Rigorous and more detailed formulation of the SPRP technique can be found in [30].

3. Antenna design using SPRP: test cases

In this section we present three antenna design examples where the geometry parameters are adjusted using the SPRP methodology described in Sec. 2. We consider a dielectric resonator antenna, a wideband microstrip antenna, as well as an ultrawideband dipole antenna.

3.1. Dielectric resonator antenna. Consider a rectangular DRA installed at a ground plane and operating at the $\text{TE}_{\delta 11}$ mode [2], see Fig. 2 for its geometry. The DRA is fed with a 50 ohm microstrip through a slot made in the ground plane. The design variables are $\boldsymbol{x} = [a_x \ a_y \ a_z \ a_{y0} \ u_s \ w_s \ y_s]^T$, where a_x, a_y, and a_z are dimensions of the dielectric resonator (DR) brick, a_{y0} stands for the shift of the DR center in Y-direction relative to the slot center, u_s is the slot width, w_s is the lot length, and y_s is the length of the microstrip stub. Relative dielectric constant and loss tangent of the DR are 10 and 1e-4 respectively. Substrate is 0.5 mm thick RO4003C material [31]. The width of the microstrip signal trace is 1.17 mm. Metallization of the trace and ground is with 50 μm copper.

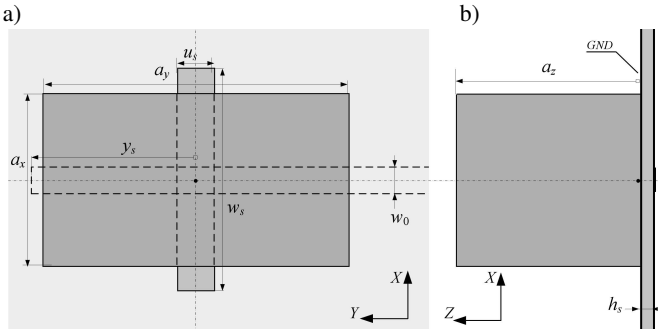

Fig. 2. DRA [2]: a) top and b) side views

The design objective for reflection coefficient is to obtain $|S_{11}| \leq -10$ dB for at least 8% fractional bandwidth centered at 5.5 GHz (5.28 GHz to 5.72 GHz). The initial design is $\boldsymbol{x}^{(0)} = [8.0 \ 14.0 \ 8.0 \ 0.0 \ 1.7 \ 8.4 \ 8.3]^T$ mm, and it is obtained for 5.5 GHz with available design guidelines and data curves of [2]. However, this initial design does not meet the specifications (dot and dash lines in Fig. 3). The design requirements concerning the DRA radiation are the following: realized gain not less than 3 dB for zero zenith angle, and realized gain in directions down the substrate (back radiation) not greater than -15 dB, both over the frequencies where $|S_{11}|$ meets the matching specifications. In the optimization process, only the $|S_{11}|$ requirements are handled directly (through the objective function), whereas the radiation

requirements are treated as constraints and included into the objective function through appropriate penalty terms.

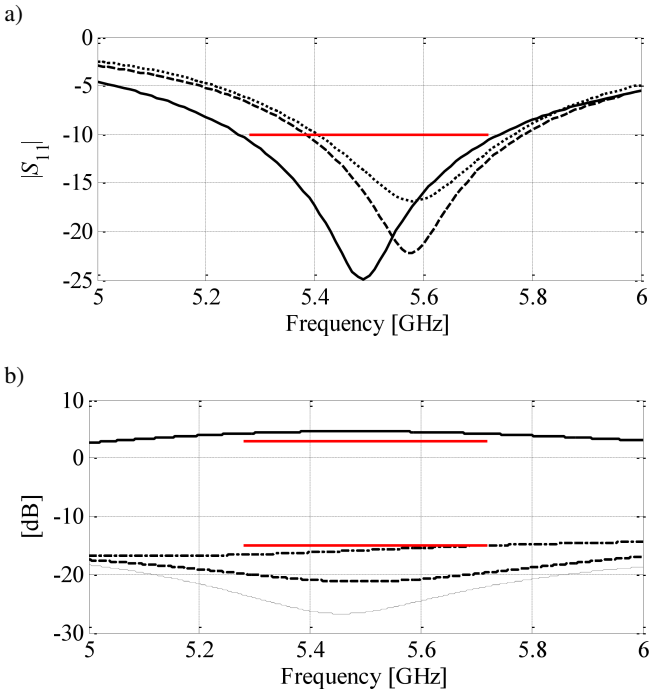

Fig. 3. DRA: a) high- (dashed line) and low-fidelity fidelity model response (dotted line) at the initial design $\boldsymbol{x}^{(0)}$, and high-fidelity (solid line) model response at the final design; b) realized gain of the DRA at the final design: for zenith angle of 0° (thick solid line); and back radiation, zenith angles of 135° (positive Y-direction, thin solid line), 180° (right down, dash line), and 135° (negative Y-direction dash-dot line). Design constrains over the bandwidth are shown with the upper horizontal line of the 3 dB level, and lower line of the -15 dB level

The high-fidelity model $\boldsymbol{R}_f$ is simulated using the CST MWS transient solver [32] (505.250 mesh cells at the initial design, 10 min 47 s of the run time). The low-fidelity model $\boldsymbol{R}_{cd}$ is also evaluated in the same solver but with coarser discretization (14,800 mesh cells at $\boldsymbol{x}^{(0)}$, 24 seconds). The final design $\boldsymbol{x}^{(2)} = [8.2\ 14.2\ 8.3\ 0.0\ 1.8\ 9.4\ 7.6]^T$ mm is obtained after two iterations of the SPRP algorithm with the total cost corresponding to about seven evaluations of the high-fidelity model (Table 1). Figure 3a shows the reflection of $\boldsymbol{R}_f$ at both the initial and the final design, as well as the response of $\boldsymbol{R}_{cd}$ at $\boldsymbol{x}^{(0)}$. Figure 3b shows the realized gain of the antenna at the final design.

Table 1
Dielectric resonator antenna: optimization cost

Algorithm component	Number of model evaluations	Evaluation time	
		Absolute [min]	Relative to $\boldsymbol{R}_f$
Evaluation of $\boldsymbol{R}_{cd}^{*}$	$105 \times \boldsymbol{R}_{cd}$	42	3.9
Evaluation of $\boldsymbol{R}_f^{\#}$	$3 \times \boldsymbol{R}_f$	32	3.0
Total optimization time	N/A	74	**6.9**

* Includes optimization of SPRP surrogate (based on $\boldsymbol{R}_{cd}$).
$^{\#}$ Includes evaluation of $\boldsymbol{R}_f$ at the initial design.

3.2. Wideband microstrip antenna. Consider an antenna shown in Fig. 4 [33] where $\boldsymbol{x} = [l_1\ l_2\ l_3\ l_4\ w_2\ w_3\ d_1\ s]^T$ are the design variables. Multilayer substrate is $l_s \times l_s$ ($l_s = 30$ mm). The antenna stack (bottom-to-top) comprises: metal ground, 0.813 mm thick RO4003, microstrip trace ($w_1 = 1.1$ mm), 1.905 mm thick RO3006 and a trace-to-patch via ($r_0 = 0.25$ mm), driven patch, 3.048 mm thick RO4003, and four patches at the top. The antenna stack is fixed with four M1.6 bolts at the corners ($u = 3$ mm). Metallization is with thick 50 μm copper. Feeding is through an edge mount 50 ohm SMA connector with the 10 mm × 10 mm × 2 mm flange.

The design objective is $|S_{11}| \leq -10$ dB for 3.1 GHz to 4.8 GHz. Realized gain not less than 5 dB for the zero zenith angle is an optimization constrain over the frequency band. The initial design is $\boldsymbol{x}^{init} = [-4\ 15\ 15\ 2\ 15\ 15\ 20\ 2]^T$ mm.

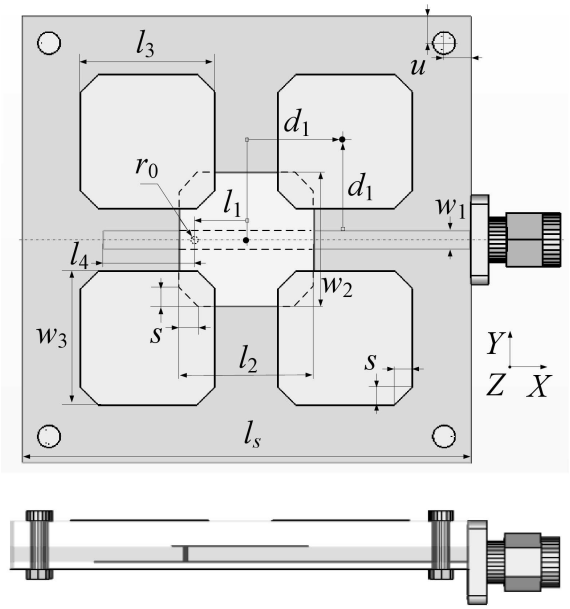

Fig. 4. Wideband microstrip antenna: top and side views. The dash-dot line in the top view shows the magnetic symmetry wall (XOY)

Both the high-fidelity model $\boldsymbol{R}_f$ (2,334,312 mesh cells at the initial design, 160 minutes of the evaluation time) and the low-fidelity model $\boldsymbol{R}_{cd}$ (122,713 mesh cells, 3 min of the evaluation time) are simulated using the CST MWS transient solver [32].

Here, the first step is to find the rough optimum of $\boldsymbol{R}_{cd}$, $\boldsymbol{x}^{(0)}$=$[-4.91\ 15.15\ 15.07\ 2.56\ 14.21\ 14.23\ 21.07\ 2.67]^T$ mm. The computational cost of this step is 82 evaluations of $\boldsymbol{R}_{cd}$ (which corresponds to about 1.5 evaluations of the high-fidelity model). Figure 5a shows the responses of $\boldsymbol{R}_f$ at $\boldsymbol{x}^{init}$ and $\boldsymbol{x}^{(0)}$, as well as the response of $\boldsymbol{R}_{cd}$ at $\boldsymbol{x}^{(0)}$.

The final design $\boldsymbol{x}^{(4)} = [-5.21\ 15.38\ 15.57\ 2.58\ 14.41\ 13.73\ 21.07\ 2.067]^T$ mm ($|S_{11}| \leq -11$ dB for 3.1 GHz to 4.8 GHz, Fig. 5b is obtained after four iterations of the SPRP-based optimization. The gain of the final design is shown in Fig. 5c which illustrates that the maximum of radiation points along the zero zenith angle closely over the bandwidth of in-

terest. The total design cost corresponds to about 10 evaluations of the high-fidelity model (Table 2).

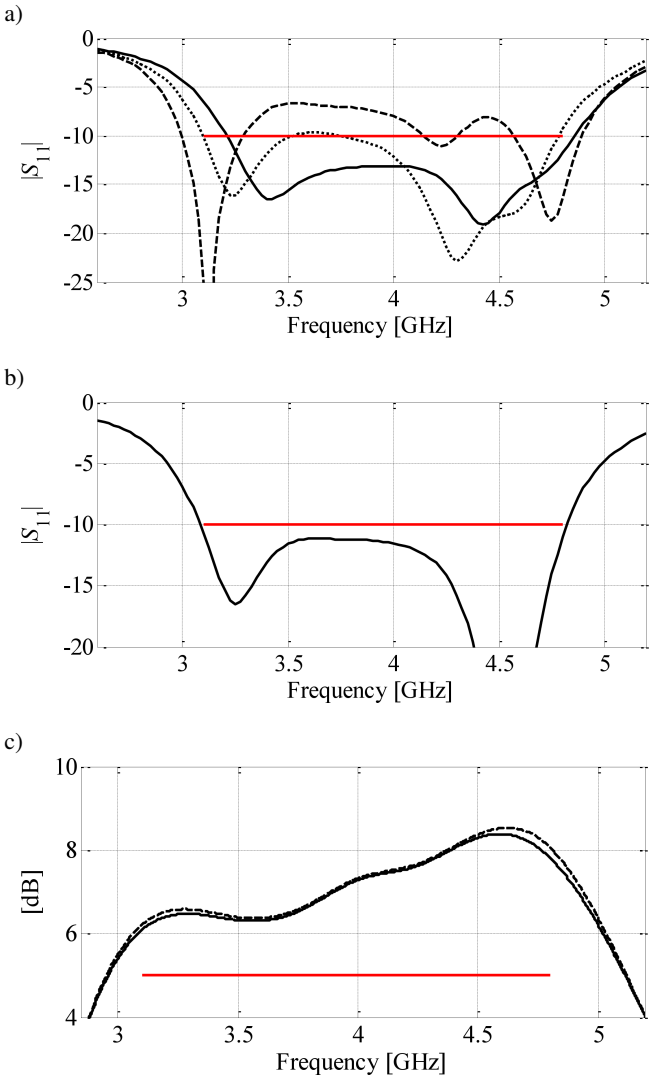

Fig. 5. Wideband microstrip antenna: a) high-fidelity model response (dashed line) at the initial design $\boldsymbol{x}^{init}$, and high- (solid line) and low-fidelity (dotted line) model responses at the approximate low-fidelity model optimum $\boldsymbol{x}^{(0)}$; b) high-fidelity model $|S_{11}|$ at the final design; c) realized gain at the final design for the zero zenith angle (solid line, XOZ co-pol.) and realized peak gain (dash line). Design constrain is shown with the horizontal line at the 5 dB level

Table 2

Wideband microstrip antenna: optimization cost

Algorithm component	Number of model evaluations	Evaluation time	
		Absolute [hours]	Relative to $\boldsymbol{R}_f$
Evaluation of $\boldsymbol{R}_{cd}^{*}$	289 × $\boldsymbol{R}_{cd}$	14.4	5.4
Evaluation of $\boldsymbol{R}_f^{\#}$	5 × $\boldsymbol{R}_f$	13.3	5.0
Total optimization time	N/A	27.7	**10.4**

* Includes optimization of $\boldsymbol{R}_{cd}$ and optimization of SPRP surrogate.

\# Excludes evaluation of $\boldsymbol{R}_f$ at the initial design.

3.3. Planar UWB dipole antenna. Consider a planar antenna shown in Fig. 6. It consists of a planar dipole as the main radiator element and two additional strips. The design variables are $\boldsymbol{x} = [l_0\ w_0\ a_0\ l_p\ w_p\ s_0]^T$. Other dimensions are fixed to: $a_1 = 0.5$ mm, $w_1 = 0.5$ mm, $l_s = 50$ mm, $w_s = 40$ mm, and $h = 1.58$ mm. Substrate material is Rogers RT5880 [34].

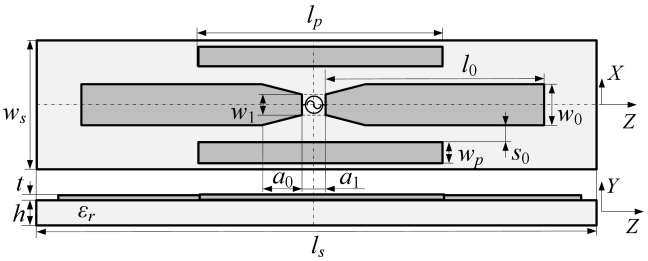

Fig. 6. UWB dipole antenna geometry: top and side views. The dash-dot lines show the electric (YOZ) and the magnetic (XOY) symmetry walls. The 50 ohm source impedance is not shown at the figure

The high-fidelity model $\boldsymbol{R}_f$ of the antenna structure (10,250,412 mesh cells at the initial design, evaluation time of 44 minutes) is simulated using the CST MWS transient solver [32]. The design objective is to obtain $|S_{11}| \leq -12$ dB for 3.1 GHz to 10.6 GHz. The initial design is $\boldsymbol{x}^{init} = [20\ 10\ 1\ 10\ 8\ 2]^T$ mm. The low-fidelity model $\boldsymbol{R}_{cd}$ is also evaluated in CST but with coarser discretization (108,732 cells at $\boldsymbol{x}^{init}$, evaluated in 43 seconds).

For this example, the approximate optimum of $\boldsymbol{R}_{cd}$, $\boldsymbol{x}^{(0)} = [18.66\ 12.98\ 0.526\ 13.717\ 8.00\ 1.094]^T$ mm, is found as the first design step. The computational cost is 127 evaluations of $\boldsymbol{R}_{cd}$, it corresponds to about two evaluations of $\boldsymbol{R}_f$. Figure 7a shows the reflection responses of $\boldsymbol{R}_f$ at both $\boldsymbol{x}^{init}$ and $\boldsymbol{x}^{(0)}$, as well as the response of $\boldsymbol{R}_{cd}$ at $\boldsymbol{x}^{(0)}$.

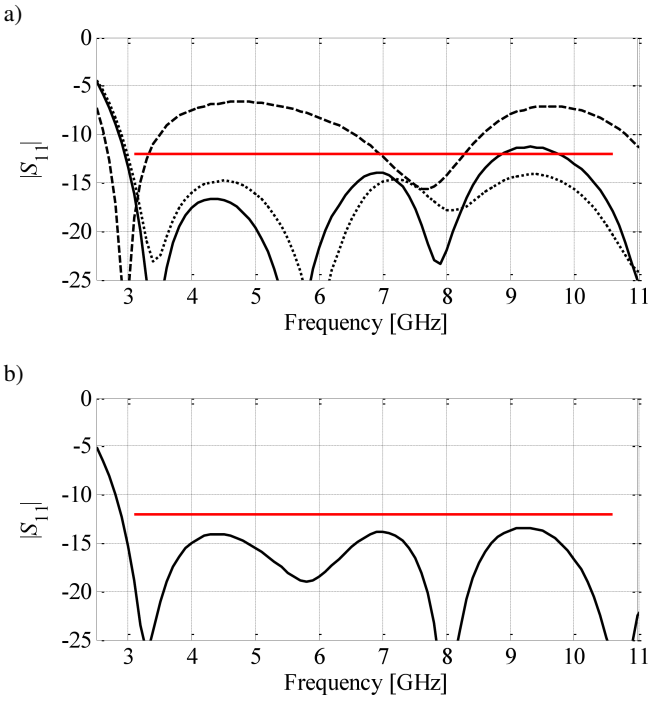

Fig. 7. UWB dipole antenna reflection response: a) high-fidelity mod-

el response (dashed line) at the initial design $\boldsymbol{x}^{init}$, and high- (solid line) and low-fidelity (dotted line) model responses at the approximate low-fidelity model optimum $\boldsymbol{x}^{(0)}$; b) high-fidelity model $|S_{11}|$ at the final design

The final design $\boldsymbol{x}^{(2)}$ = [19.06 12.98 0.426 13.52 6.80 1.094]^T mm ($|S_{11}| \leq -13.5$ dB for 3.1 GHz to 10.6 GHz) is obtained after two iterations of the SPRP-based optimization with the total cost corresponding to about 7 evaluations of the high-fidelity model (see Table 3). Figure 7b shows the reflection response and Fig. 8 shows the gain response of the final design $\boldsymbol{x}^{(2)}$.

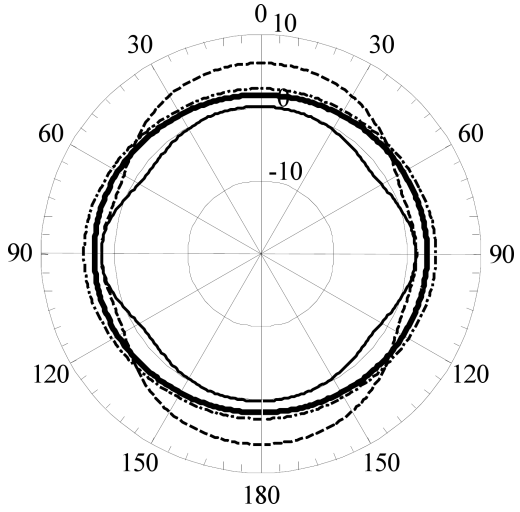

Fig. 8. UWB dipole antenna at the final design: IEEE gain pattern ($\times$-pol.) in the XOY plane at 4 GHz (thick solid), 6 GHz (dash-dot line), 8 GHz (dash line), and 10 GHz (solid line)

Table 3
UWB dipole antenna: optimization cost

Algorithm component	Number of model evaluations	Evaluation time	
		Absolute [min]	Relative to $\boldsymbol{R}_f$
Evaluation of $\boldsymbol{R}_{cd}^{*}$	233 $\times$ $\boldsymbol{R}_{cd}$	167	3.8
Evaluation of $\boldsymbol{R}_{f}^{\#}$	3 $\times$ $\boldsymbol{R}_f$	132	3.0
Total optimization time	N/A	299	**6.8**

* Includes initial optimization of $\boldsymbol{R}_{cd}$ and optimization of SPRP surrogate.
$^{\#}$ Excludes evaluation of $\boldsymbol{R}_f$ at the initial design.

3.4. Discussion. The presented examples demonstrated efficiency of the shape-preserving response prediction technique for adjusting geometry parameters of antenna structures. An important advantage of the SPRP technique is that its surrogate model does not use any extractable parameters so that the computational overhead related to multiple evaluations of the low-fidelity model is limited, compared to, e.g., space mapping. This is important because low-fidelity antenna models are typically relatively expensive as discussed in Subsec. 2.3.

In all examples the optimized design was obtained at the cost corresponding to a few evaluations of the high-fidelity model (7 to 10, depending on the example). Having in mind that finding a rough optimum of the low-fidelity model required about 80–130 $\boldsymbol{R}_{cd}$ evaluations (again, depending on the example), the cost of direct high-fidelity model optimization can be estimated as 200 or more $\boldsymbol{R}_f$ evaluations. This means that the design using the SPRP technique results in time saving at the level of 95% that is significant.

4. Conclusions

Computationally efficient simulation-driven design optimization of antennas was presented. Our approach combines coarse-discretization EM antenna models with the shape-preserving response prediction technique to create a fast and yet accurate surrogate that replaces the original, high-fidelity antenna model in the design process. We demonstrated three design cases: dielectric resonator antenna, wideband microstrip antenna, and UWB dipole antenna. In all cases, the optimized design was found at the cost corresponding to a few evaluations of the high-fidelity antenna model.

Acknowledgements. The authors thank CST AG, Darmstadt, Germany, for making CST Microwave Studio available. This work was partly supported by Icelandic Centre for Research (RANNIS) under Grant 110034021.

REFERENCES

[1] J.L. Volakis, *Antenna Engineering Handbook*, McGraw-Hill, New York, 2007.
[2] A. Petosa, *Dielectric Resonator Antenna Handbook*, Artech House, New York, 2007.
[3] H. Schantz, *The Art and Science of Ultrawideband Antennas*, Artech House, New York, 2005.
[4] C.A. Balanis, *Antenna Theory: Analysis and Design*, 3^{rd} ed., Wiley, London, 2005.
[5] J.W. Bandler, Q.S. Cheng, S.A. Dakroury, A.S. Mohamed, M.H. Bakr, K. Madsen, and J. Søndergaard, "Space mapping: the state of the art", *IEEE Trans. Microwave Theory Tech.* 52 (1), 337–361 (2004).
[6] J.M. Johnson and Y. Rahmat-Samii, "Genetic algorithms in engineering electromagnetics", *IEEE Antennas Propag. Mag.* 39 (4), 7–21 (1997).
[7] A.J. Kerkhoff and H. Ling, "Design of a band-notched planar monopole antenna using genetic algorithm optimization", *IEEE Trans. Antennas Propag.* 55 (3), 604–610 (2007).
[8] R.L. Haupt, "Antenna design with a mixed integer genetic algorithm", *IEEE Trans. Antennas Prop.* 55 (3), 577–582 (2007).
[9] M. John and M.J. Ammann, "Wideband printed monopole design using a genetic algorithm", *IEEE Antennas Wireless Propag. Lett.* 6, 447–449 (2007).
[10] L. Lizzi, F. Viani, R. Azaro, and A Massa, "Optimization of a spline-shaped UWB antenna by PSO", *IEEE Antennas Wireless Propag. Lett.* 6, 182–185 (2007).
[11] N. Jin and Y. Rahmat-Samii, "Analysis and particle swarm optimization of correlator antenna arrays for radio astronomy applications", *IEEE Trans. Antennas Propag.* 56 (5), 1269–1279 (2008).
[12] M. Donelli and A. Massa, "Computational approach based on a particle swarm optimizer for microwave imaging of two-dimensional dielectric scatterers", *IEEE Trans. Microw. Theory Tech.* 53, 1761–1776 (2005).
[13] A. Halehdar, D.V. Thiel, A. Lewis, and M. Randall, "Multi-objective optimization of small meander wire dipole antennas in a fixed area using ant colony system", *Int. J. RF and Microwave CAE* 19 (5), 592–597 (2009).

[14] N.V. Queipo, R.T. Haftka, W. Shyy, T. Goel, R. Vaidynathan, and P.K. Tucker, "Surrogatebased analysis and optimization", *Progress in Aerospace Sciences* 41 (1), 1–28 (2005).

[15] A.I.J. Forrester and A.J. Keane, "Recent advances in surrogate-based optimization", *Prog. in Aerospace Sciences* 45 (1–3), 50–79 (2009).

[16] H. Kabir, Y. Wang, M. Yu, and Q.J. Zhang, "High-dimensional neural-network technique and applications to microwave filter modeling", *IEEE Trans. Microwave Theory Tech.* 58 (1), 145–156 (2010).

[17] Y. Tighilt, F. Bouttout, and A. Khellaf, "Modeling and design of printed antennas using neural networks", *Int. J. RF and Microwave CAE* 21 (2), 228–233 (2011).

[18] L. Xia, J. Meng, R. Xu, B. Yan, and Y. Guo, "Modeling of 3-D vertical interconnect using support vector machine regression", *IEEE Microwave Wireless Comp. Lett.* 16 (12), 639–641 (2006).

[19] M. Martinez-Ramon and C. Christodoulou, "Support vector machines for antenna array processing and electromagnetics", *Synthesis Lectures on Computational Electromagnetics* 1 (1), 77–81 (2006).

[20] V. Miraftab and R.R. Mansour, "EM-based microwave circuit design using fuzzy logic techniques" *IEE Proc. Microwaves, Antennas & Propagation* 153 (6), 495–501 (2006).

[21] J. Zhai, J. Zhou, L. Zhang, and W. Hong, "Behavioral modeling of power amplifiers with dynamic fuzzy neural networks", *IEEE Microwave and Wireless Comp. Lett.* 20 (9), 528–530 (2010).

[22] G.S.A. Shaker, M.H. Bakr, N. Sangary, and S. Safavi-Naeini "Accelerated antenna design methodology exploiting parameterized Cauchy models", *J. Progress in Electromagnetic Research (PIER B*) 18, 279–309 (2009).

[23] E.S. Siah, M. Sasena, J.L. Volakis, P.Y. Papalambros, and R.W. Wiese, "Fast parameter optimization of large-scale electromagnetic objects using DIRECT with Kriging metamodeling", *IEEE Trans. Microwave Theory Tech.* 52 (1), 276–285 (2004).

[24] I. Couckuyt, F. Declercq, T. Dhaene, H. Rogier, and L. Knockaert, "Surrogate-based infill optimization applied to electromagnetic problems", *Int. J. RF and Microwave CAE* 20 (5), 492–501 (2010).

[25] S. Amari, C. LeDrew, and W. Menzel, "Space-mapping optimization of planar coupled-resonator microwave filters", *IEEE Trans. Microwave Theory Tech.* 54 (5), 2153–2159 (2006).

[26] G. Crevecoeur, L. Dupre, and R. Van de Walle, "Space mapping optimization of the magnetic circuit of electrical machines including local material degradation", *IEEE Trans. Magn.* 43 (6), 2609–2611 (2007).

[27] S. Koziel, Q.S. Cheng, and J.W. Bandler, "Space mapping", *IEEE Microwave Magazine* 9 (6), 105–122 (2008).

[28] J.C. Rautio, "EM-component-based design of planar circuits", *IEEE Microwave Magazine* 8 (4), 79–90 (2007).

[29] S. Koziel, J. Meng, J.W. Bandler, M.H. Bakr, and Q.S. Cheng, "Accelerated microwave design optimization with tuning space mapping", *IEEE Trans. Microwave Theory and Tech.* 57 (2), 383–394 (2009).

[30] S. Koziel, "Shape-preserving response prediction for microwave design optimization", *IEEE Trans. Microwave Theory and Tech.* 58 (11), 2829–2837 (2010).

[31] *RO4000®Series High Frequency Circuit Materials*, *Data Sheet*, Rogers Corporation, Publication #92-004, 2010.

[32] CST Microwave Studio, ver. 2010, *CST AG*, Bad Nauheimer Str. 19, D-64289 Darmstadt, 2010.

[33] Z.N. Chen, "Wideband microstrip antennas with sandwich substrate", *IET Microw. Ant. Prop*. 2 (6), 538–546 (2008).

[34] *RT/duroid®5870 /5880 High Frequency Laminates*, *Data Sheet*, Rogers Corporation, Publication #92-101, 2010.